THE SYNCHROTRON RADIATION BEAMLINE AT TTF2

S. Casalbuoni, L. Fröhlich, O. Grimm*, O. Peters, J. Rossbach, DESY, Hamburg, Germany

Abstract

At the DESY TTF2 linear accelerator that will drive the VUV-FEL, a beamline to transport visible and far-infrared synchrotron radiation from the first bunch compressor to a diagnostic station outside the tunnel has been constructed. The purpose is to use a streak camera and spectral analysis in the far-infrared to measure the longitudinal bunch shape.

BEAMLINE LAYOUT

General

The VUV-FEL at DESY, Hamburg, will require novel techniques to characterize the longitudinal charge distribution of the electron bunches that drive the free-electron laser. Conventional methods are inadequate at the short bunch lengths that will be obtained. One technique under study uses coherent far-infrared radiation to reconstruct the bunch shape through Fourier analysis of the spectrum. In a first step, a beam line to guide both far-infrared (50–3000 μm) and optical synchrotron radiation from the first bunch compressor (BC2) of the TTF2 linear accelerator to a diagnostic station outside of the controlled area at some 10 m distance has been constructed. It will allow a direct comparison between streak camera and far-infrared measurements for features on length scales above some 100 μm (the streak camera resolution). Later, infrared techniques extending to shorter wavelengths, i.e. to shorter bunch lengths, will also be used further downstream the accelerator, employing synchrotron, transition and undulator radiation.

The principle design of the beamline relies on simple optics: a paraboloid mirror close to the synchrotron radiation viewport transforms radiation originating from an arc of about 7 cm length in the source region at some 81 cm distance into a nearly parallel beam which is then transported by large flat mirrors through Aluminium pipes to the experimental station. The beamline including the interferometer is flushed with dry Nitrogen to reduce the strong absorption of water vapour in the far-infrared. It is already partly prepared for later evacuation to fore-vacuum in case the absorption needs to be reduced further. A crystalline Quartz window (z-cut, clear aperture ⌀60 mm, 4.8 mm thick) is used as viewport. Photos of the beamline are shown in Fig. 1.

Outcoupling port

The synchrotron port at the fourth BC2 magnet (D4BC2) is at 18° relative to the beam axis, looking at approximately

---
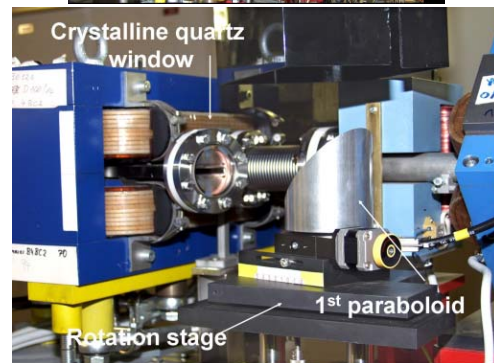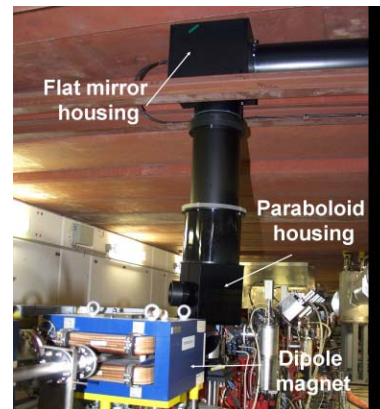
Figure 1: Photographs showing an overview of the beamline in the tunnel (left) and the outcoupling port (right).

the first 2.5° of the beam trajectory arc. With a nominal bending radius of about 1.6 m at 130 MeV, this corresponds to an arc length of 7.0 cm. The geometry for this setting is sketched in Fig. 2.
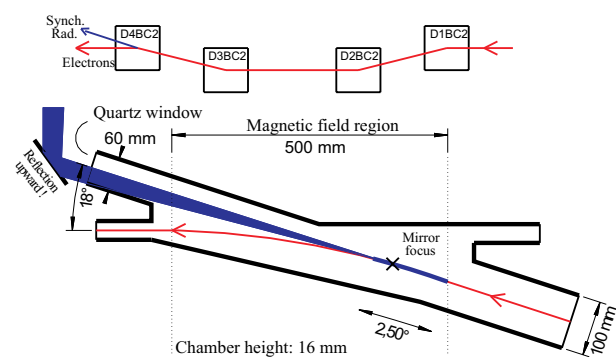
Figure 2: BC2 layout and D4BC2 vacuum chamber.

The radiation is emitted along this arc into a cone of typical half-opening angle of 2.4°(42 mrad) at 250 μm and of 0.2°(3.5 mrad) at 500 nm. In the vertical the radiation beam is restricted by the vacuum chamber height of 16 mm, in

---

* Corresponding author. E-Mail: oliver.grimm@desy.de

the horizontal by the 60 mm diameter window. To transport this beam over some 10 m distance requires focusing of the infrared radiation soon after the chamber window to limit the necessary mirror sizes. To this end, a 90°off-axis paraboloid mirror is installed after the window, its focal point being 5 cm away from the beginning of the arc, and reflecting the parallelized beam upwards to the tunnel roof.

The paraboloid is machined from Aluminium, has a projected diameter of 100 mm and 810 mm focal length. The surface peak-to-valley is about 5 µm at the edge, improving towards the centre. The surface quality is limited due to difficulties in machining the large focal length. This has the effect of broadening the spot of visible radiation after the beamline, requiring further focusing into the streak camera, but does not influence the performance in the far-infrared.

The paraboloid will correctly parallelize only radiation originating at its focus. Radiation originating at the beginning of the arc will converge over 10 m to about half its initial diameter (100 mm, given by the paraboloid size). Radiation originating closer will diverge slightly. It is possible to manually move the paraboloid focal point by +5 cm/-2 cm to optimize the beam transport.

Depending on the bunch compressor settings, the electron beam can enter the dipole chamber at any position allowed by its width of 100 mm. The mirror can be rotated around its vertical axis, such that the focus follows the emission region of the synchrotron radiation transversely. The rotation plane is aligned with the nominal electron beam plane. The focusing is not very sensitive to the exact longitudinal position, so that no translation of the mirror is necessary.

Transport line

The approximately parallel beam from the paraboloid is reflected by an Aluminium flat mirror ($\varnothing$ 250 mm) under the tunnel roof straight out to two further standard flat mirrors ($\varnothing$ 152.4 mm, Aluminium coating on pyrex substrate) in the diagnostic container that feed the radiation into the interferometer. Switching to the streak camera is done with a number of smaller mirrors (since only the visible component with smaller opening angle is used), a lens and suitable, narrow wavelength filters. The beam travels within black anodized Aluminium pipes of 250 mm diameter (200 mm over a short section through the radiation protection wall). Nitrogen is flushed from the diagnostic station into the tunnel at flow rates below 1 l/s, so that effluence into the tunnel is of no security concern.

Reflection of linear polarized light from a metallic mirror will, in general, result in elliptical polarization, depending on the angle of incidence and initial polarization. For an Aluminium mirror in the far-infrared, however, the situation is simpler. The component polarized parallel to the plane of incidence will suffer no phase shift, the orthogonal component a shift of 180°for angles of incidence not too close to 90°. In effect, if the initial polarization has an angle α to the plane of incidence, it will have an angle $-\alpha$

after reflection. The emitted synchrotron radiation will be polarized almost completely in the (horizontal) electron orbital plane, as the vertical opening angles are small. The polarization plane will then be preserved in space if the radiation beam travels again parallel to its initial direction after a number of reflections.

Interferometer

A polarizing Martin-Puplett interferometer[1], shown in Fig. 3, is used to analyze the spectrum of the far-infrared radiation. The grids are wound from 10 µm gold-plated Tungsten wire with 30 µm spacing. Currently, DTGS pyroelectric detectors are used, a liquid Helium cooled bolometer is also available. Details of the device can be found in [1, Chapter 7]. The input polarizer, implemented since the interferometer was originally used with transition radiation, is not necessary for synchrotron radiation, but can be used to measure the degree of polarization.

Compared to a Michelson interferometer, this type has the advantage of an almost perfect beam splitter characteristic for wavelengths longer than about twice the wire spacing and full transmission of the incoming radiation to the detectors (whereas on average half is reflected back to the source with a Michelson device). This allows an easy correction for fluctuations in the incoming intensity.
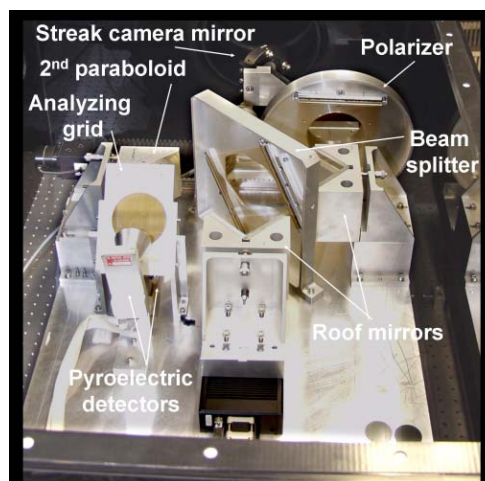
Figure 3: The Martin-Puplett interferometer.

FIRST RESULTS

During the first run of TTF2 in May/June 2004, the infrared beamline was commissioned and first interferograms were taken. Fig. 4 shows one example. Clearly visible is one advantage of the Martin-Puplett interferometer: it allows suppression of radiation intensity fluctuations by normalizing the detector signals to the total intensity, i.e. their sum. Such fluctuations were strong during this startup phase.

---

[1] Build by RWTH Aachen.
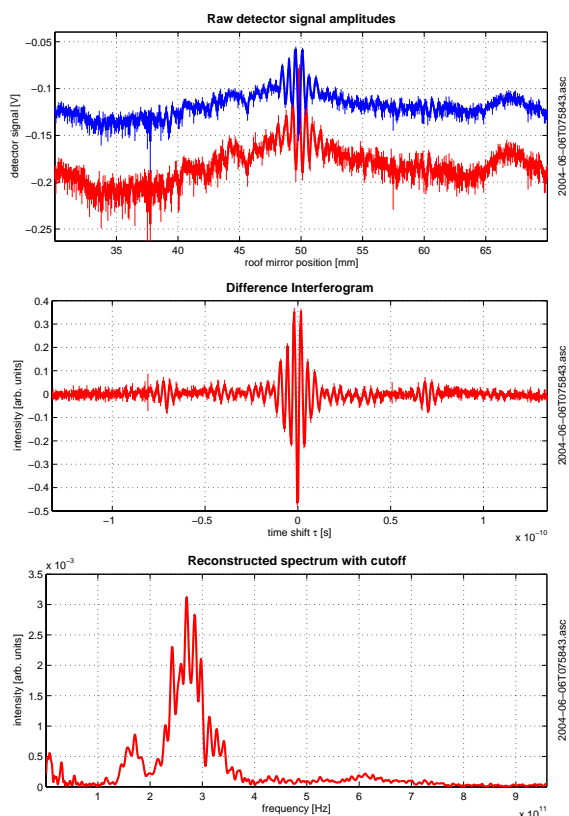
Figure 4: Measured raw (top) and normalized difference (middle) interferogram and the reconstructed spectrum (bottom) from the first run of TTF2 in May/June 2004.

The interferogram shows a small secondary signal at about 67 ps delay, coming from reflections within the 4.8 mm thick Quartz window, also reflected in the spectrum by the interference structure. The spectral shape shows general agreement with the first simulations (see below), but more detailed analysis is necessary to extract quantitative information. A first estimate of the degree of polarization gave a value in excess of 90%.

ANALYSIS

The bunch shape is imprinted on the spectrum through the form factor $F(\lambda)$,

$$\frac{\mathrm{d}U}{\mathrm{d}\lambda} = \left(\frac{\mathrm{d}U}{\mathrm{d}\lambda}\right)_0 \left(N + N(N-1) |F(\lambda)|^2\right), \quad (1)$$

where $(\mathrm{d}U/\mathrm{d}\lambda)_0$ is the emission spectrum of one single electron, N is the total number of electrons and the form factor is the Fourier transform of the normalized longitudinal charge distribution $S(z)$,

$$F(\lambda) = \int_{-\infty}^{\infty} S(z) \exp\left(\frac{-2\pi\mathrm{i}}{\lambda} z\right) \mathrm{d}z. \quad (2)$$

The final goal is to reconstruct the charge distribution from the measured spectrum via the technique of Kramers-Kronig analysis to retrieve the missing phase information

for the inverse Fourier transform [2]. This will require precise knowledge of spectral modifications by the vacuum chambers, beam line, interferometer and detectors and a critical extrapolation of the measured data.

At the current state of the experiment, the opposite way has been pursued. Simulations are performed to calculate the expected spectrum. An example where the actual magnetic field of the fourth BC2 magnet, the vacuum chamber cut-off (see [3]) and the form factor for three bunch shapes has been taken into account is shown in Fig. 5. A parametrization for the two sharply peaked shapes is given in [4]. Not yet included is the transmission characteristic of the beamline which is currently under study using optical simulation software and the frequency response of the pyroelectric detector. Interference with radiation from the third magnet will modify the spectrum, but also requires further understanding of the beamline optics and has been neglected in this example.
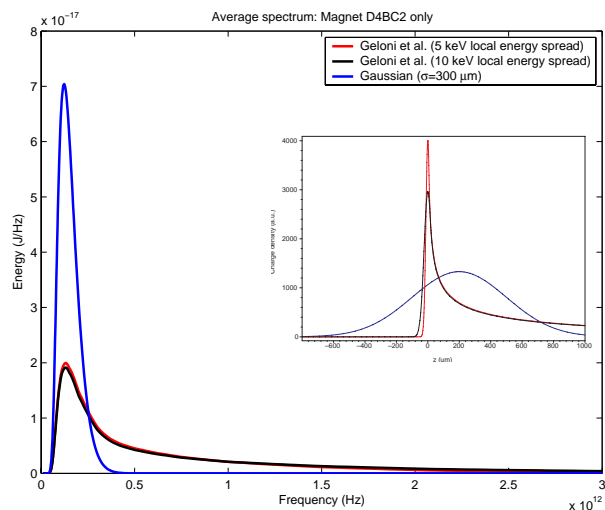
Figure 5: Simulated spectrum including form factor for the bunch shapes shown in the inset, chamber cut-off and window transmission.

REFERENCES

[1] M.A. Geitz, DESY-THESIS-1999-033 (November 1999)

[2] R. Lai, A.J. Sievers, Nucl. Instr. Meth. A397(1997) 221

[3] M. Dohlus, T. Limberg, Nucl. Instr. Meth. A407(1998) 278

[4] G. Geloni et al., DESY 03-031 (March 2003)